

# The Energy-Loss Spectrum

# 38

---

<b>38.1. A Few Basic Concepts</b> .....	<b>655</b>
<b>38.2. The Zero-Loss Peak</b> .....	<b>656</b>
<b>38.3. The Low-Loss Spectrum</b> .....	<b>656</b>
<b>38.3.A. Plasmons</b> .....	<b>656</b>
<b>38.3.B. Inter- and Intra-Band Transitions</b> .....	<b>658</b>
<b>38.4. The High-Loss Spectrum</b> .....	<b>658</b>
<b>38.4.A. Inner-Shell Ionization</b> .....	<b>658</b>
<b>38.4.B. Ionization-Edge Characteristics</b> .....	<b>662</b>
<b>38.5. Artifacts in the Spectrum</b> .....	<b>664</b>

## CHAPTER PREVIEW

The term “energy-loss” spectrometry implies that we are only interested in inelastic interactions, but the spectrum will also contain electrons which have not lost any energy so we need to consider elastic scattering as well. We’ll deal with three principal regions of the energy-loss spectrum:

- The zero-loss peak, which consists primarily of elastic forward-scattered electrons, but also contains electrons that have suffered minor (unresolvable) energy losses.
- The low-loss region up to an energy loss of ~50 eV contains electrons which have interacted with the weakly bound outer-shell electrons of the atoms in the specimen.
- Electrons in the high-loss region have interacted with the more tightly bound inner-shell or “core” electrons.

These different regimes of energy losses can give us different information about the specimen. The terminology is a bit vague but is generally accepted. The zero-loss peak defines the energy resolution and is essential in calibrating your spectrum. The electrons in the low-loss region have only interacted weakly with the atoms via their outer-shell electrons, so they contain information about the electronic properties of the specimen. The electrons in the high-loss region have “probed” the inner electron shells and therefore contain information characteristic of the atoms in the specimen.

We can also obtain information about how the atoms are bonded to one another, and even how the neighboring atoms are distributed around a specific atom. In principle, the energy-loss spectrum is far more useful than an XEDS spectrum. However, it is also far more complex. To understand its content you need a greater understanding of the physics of beam–specimen interactions. The spectrum also contains artifacts which we need to identify and minimize.

In this chapter we will discuss the different features of electron energy-loss spectra and go on to use these spectra in Chapters 39 and 40.

# The Energy-Loss Spectrum

# 38

## 38.1. A FEW BASIC CONCEPTS

Back in Chapters 2–4 we talked about the difference between elastic and inelastic beam–specimen interactions and introduced the ideas of scattering cross sections and the associated mean-free path. It would be a good idea to remind yourself of those ideas before starting on this chapter. Briefly, you should recall that elastic scattering is an electron–nucleus interaction; the word “elastic” implies that there is no energy loss although a change in direction, and hence in momentum, usually occurs. Elastic scattering is usually manifest as Bragg diffraction in crystalline specimens. Inelastic scattering is primarily an electron–electron interaction and entails both a loss of energy and a change of momentum. Therefore, we have to be concerned with both the amount of energy lost and the direction of the electrons after they’ve come through the specimen. This latter point is one reason why the collection semiangle of the spectrometer is so important.

Remember, the cross section is a measure of the probability of a specific scattering event occurring and the mean free path is the average distance between particular interactions. Also, you must remember to distinguish between the definitions of scattering that will keep appearing.

Single scattering occurs when each electron undergoes at most one scattering event as it traverses the specimen.

Plural scattering (>1 scattering event) and multiple scattering (>20 scattering events) imply that the electron has undergone a combination of interactions.

We’ll see that the energy-loss spectrum is most understandable when it represents single scattering. This ideal is approached when we have very thin specimens. In prac-

tice, most specimens are thicker than ideal and so we usually acquire plural-scattering spectra, and we may have to remove the plural-scattering effects. If multiple scattering occurs, the specimen is too thick for EELS and for much of TEM in general.

The principal inelastic interactions in order of increasing importance (and energy loss) are phonon excitations, inter- and intra-band transitions, plasmon excitations, and inner-shell ionizations. We’ve already introduced these processes back in Chapter 4 and we will emphasize inner-shell ionizations almost exclusively from here on. The two major characteristics of any inelastic scattering are the energy loss  $\mathcal{E}$  and the scattering semiangle  $\theta$ , and we summarize typical values in Table 38.1.

It’s a little difficult to be specific about the values of the scattering angle because the angle varies with energy. In fact there are different definitions of scattering angle which you may come across, and these can be confusing. You can find derivations of the equations governing scattering in Egerton (1996).

The symbol  $\theta$  in all cases refers to the scattering semiangle.

We will always assume that the scattering is symmetrical around the direct beam. The most important angle is  $\theta_E$ , the so-called characteristic or most-probable scattering semiangle for an energy loss,  $\mathcal{E}$ . This angle is given by

$$\theta_E \approx \frac{\mathcal{E}}{2E_0} \quad [38.1]$$

This equation is an approximation and it ignores relativistic effects, so you should only use it for rough calculations at and above 100 keV. We can be more precise and define  $\theta_E$  as

**Table 38.1. Characteristics of the Principal Energy-Loss Processes**

Process	Energy loss (eV)	$\theta_E$ (mrads)
Phonons	~0.02	5–15
Inter/intra-band transitions	5–25	5–10
Plasmons	~5–25	<~0.1
Inner-shell ionization	~10–1000	1–5

$$\theta_E \approx \frac{\mathcal{E}}{(\gamma m_0 v^2)} \quad [38.2]$$

Here we have the usual definitions:  $m_0$  is the rest mass of the electron,  $v$  is the electron velocity, and  $\gamma$  is given by

$$\gamma = \left(1 - \frac{v^2}{c^2}\right)^{-\frac{1}{2}} \quad [38.3]$$

The electron velocity is  $v$  and  $c$  is the velocity of light. One other useful angle,  $\theta_C$ , is the cut-off angle above which the scattered intensity is zero, and this is given by

$$\theta_C = (2\theta_E)^{\frac{1}{2}} \quad [38.4]$$

In Table 38.1 we have given some typical values of  $\theta_E$ . This is the scattering angle that we'll usually refer to from now on. Let's now move on to the energy-loss spectrum. We'll start at the low-energy end and proceed to higher-energy losses.

## 38.2. THE ZERO-LOSS PEAK

If your specimen is thin, the predominant feature in the energy-loss spectrum will be the zero-loss peak. As the name implies, this peak consists mainly of electrons that have completely retained the beam energy  $E_0$ . Such electrons may be forward scattered in a relatively narrow cone within a few mrads of the optic axis and constitute the 000 spot in the DP, i.e., the direct beam. If we were to tilt the incident beam so a diffracted beam entered the spectrometer, then it too would give a zero-loss peak. The scattering angles for diffraction ( $2\theta_B$ ) are relatively large (~20 mrad) compared to the smaller collection angles in EELS, and so the diffracted beams rarely enter the spectrometer. Actually, we can also measure the intensity and energy of electrons as a function of their angular distribution, and we'll discuss this aspect briefly in Chapter 40.

Now the term “zero-loss peak” is really a misnomer for two reasons. First, our spectrometers have a finite energy resolution (at best ~0.3 eV) so the zero-loss peak will also contain electrons that have lost very small amounts of energy, mainly those that excited phonons. So in EELS in

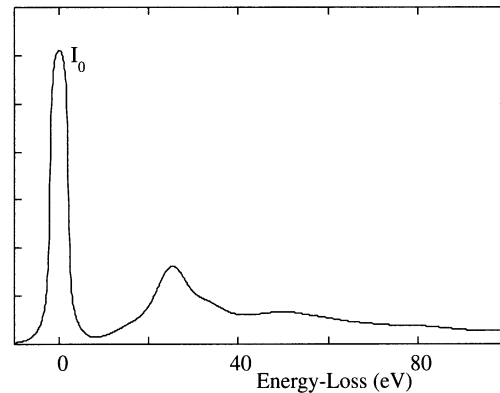


**Figure 38.1.** The intense zero-loss peak  $I_0$  in a spectrum from stainless steel. The rest of the spectrum comprises energy-loss electrons which constitute a relatively small fraction of the total intensity in the spectrum.

the TEM we never resolve phonon losses. This is not a “great loss” since phonon-loss electrons don’t carry any useful information anyway; they only cause the specimen to heat up. However, it does explain why we shouldn’t really call this the zero-loss peak. Second, we can’t produce a beam of monochromatic electrons; the beam has a finite energy range about the nominal value  $E_0$ . Despite this imprecision, we will continue to use the zero-loss terminology.

The zero-loss peak is usually a problem rather than a useful feature in the spectrum, because it is so intense that it can damage the scintillator or saturate the photodiode array. We don’t collect it except under certain circumstances. Figure 38.1 shows the intense zero-loss peak in a spectrum. To the right of the peak is a relatively small peak, which is part of the low-loss spectrum. This small peak is where we start to get useful information, but you can also see immediately that the useful part of the spectrum is very much less intense than the somewhat useless zero-loss peak, and this is one of several fundamental problems in EELS.

## 38.3. THE LOW-LOSS SPECTRUM

We use the term “low-loss” to describe energy-loss electrons in the range up to about 50 eV. In this part of the spectrum we come across electrons that have set up plasmon oscillations or have generated inter- or intra-band transitions. Plasmons are by far the most important, so we’ll look at these first.

### 38.3.A. Plasmons

Plasmons are longitudinal wave-like oscillations of weakly bound electrons. The oscillations are rapidly damped, typi-

**Table 38.2. Plasmon Loss Data for 100-keV Electrons for Several Elements**

Material	$\mathcal{E}_p$ (calc) (eV)	$\mathcal{E}_p$ (expt) (eV)	$\theta_E$ (mrad)	$\theta_C$ (mrad)	$\lambda_p$ (calc) (nm)
Li	8.0	7.1	0.039	5.3	233
Be	18.4	18.7	0.102	7.1	102
Al	15.8	15.0	0.082	7.7	119
Si	16.6	16.5	0.090	6.5	115
K	4.3	3.7	0.020	4.7	402

cally having a lifetime of about  $10^{-15}$  s and so are quite localized to  $<10$  nm. The plasmon peak is the second most dominant feature of the energy-loss spectrum after the zero-loss peak. The small peak beside the zero-loss peak in Figure 38.1 is a plasmon peak.

The energy  $\mathcal{E}_p$  lost by the beam electron when it generates a plasmon of frequency  $\omega_p$  is given by

$$\mathcal{E}_p = \frac{\hbar}{2\pi} \omega_p = \frac{\hbar}{2\pi} \left( \frac{ne^2}{\epsilon_0 m} \right)^{\frac{1}{2}} \quad [38.5]$$

where  $\hbar$  is Planck's constant,  $e$  and  $m$  are the electron charge and mass,  $\epsilon_0$  is the permittivity of free space, and  $n$  is the free-electron density. Typical values of  $\mathcal{E}_p$  are in the range 5–25 eV and a summary is given in Table 38.2.

Plasmon losses dominate in materials with free-electron structures, such as Li, Na, Mg, and Al, but occur to a greater or lesser extent in all materials.

We even see a plasmon-like peak in spectra from materials with no free electrons (such as polymers) for reasons that are not well understood. From equation 38.5 you can see that  $\mathcal{E}_p$  is affected by  $n$ , the free-electron density. Interestingly,  $n$  may change with the chemistry of the specimen. So in principle, measurement of the plasmon energy loss can give indirect microanalytical information, as we'll see later in Section 40.2. Plasmon-loss electrons also carry contrast information and therefore are important because they limit image resolution through chromatic aberration. We can remove them from the image by energy filtering, as we'll also describe in Section 40.3.

Because of the low values of  $\lambda_p$ , the characteristic scattering angles  $\theta_E$  are very small, being typically  $<0.1$  mrad (as listed in Table 38.2). So, plasmon-loss electrons are strongly forward-scattered. Their cut-off angle  $\theta_C \sim 100 \theta_E$ . Hence if you use a  $\beta$  of only 10 mrad, you will gather virtually all the plasmon-loss electrons. Also, their line width  $\Delta\mathcal{E}_p$  is at most a few eV.

A typical value of the plasmon mean-free path  $\lambda_p$  at AEM voltages is about 100 nm, and so it is reasonable to expect at least one strong plasmon peak in all but the thinnest specimens. Likewise, the number of individual losses should increase with the thickness of the specimen. Figure 38.2 shows the plasmon-loss spectra from thin and thick foils of pure Al. Since Al is a good approximation to a free-electron metal, the plasmon-loss process is the dominant energy-loss event. Plural plasmon scattering in thicker foils is a most important phenomenon because it eventually limits the interpretation of part of the spectrum containing chemical information from ionization losses in which we are really interested (see Section 38.4). The well-known properties of plasmon

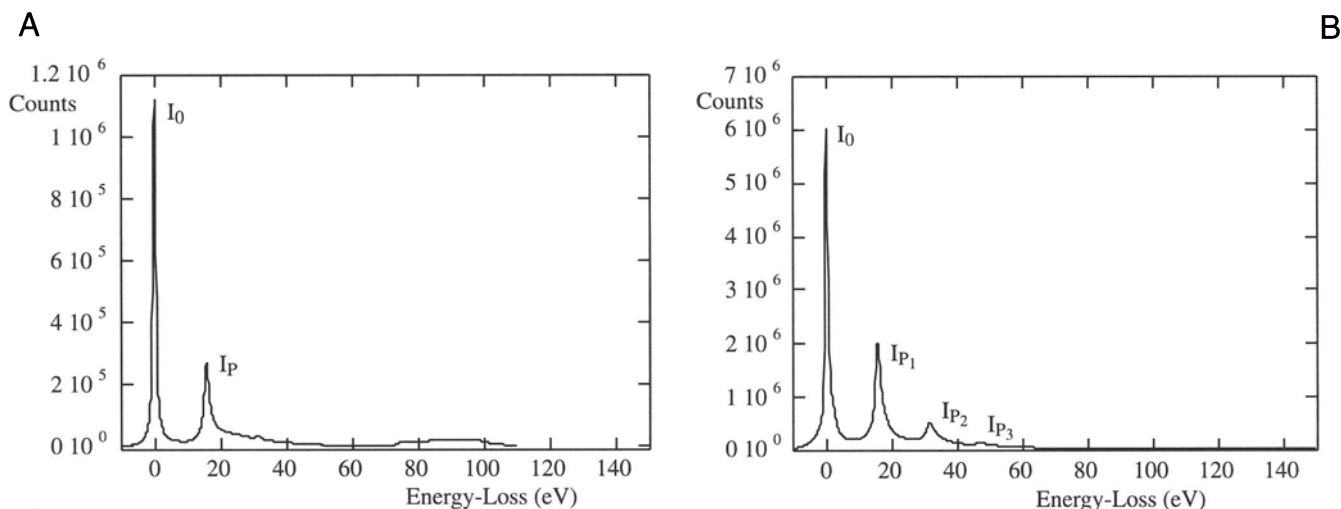


**Figure 38.2.** (A) The low-loss spectrum from a very thin sample of pure Al showing the intense zero-loss peak ( $I_0$ ) and a small plasmon peak ( $I_p$ ) at about 15 eV. (B) The low-loss spectrum from a thicker specimen of pure Al showing several plasmon peaks.

loss electrons from several elements are summarized in Table 38.2.

The plasmon losses which we've just described all arise from interactions with the electrons in the interior of the specimen, but the incident electrons can also set up plasmon oscillations on the surface of the specimen. We can envisage these surface plasmons as transverse charge waves. Surface plasmons have about half the energy of bulk plasmons. Generally, however, the surface plasmon peak is much less intense than the volume plasmon peaks, even in the thinnest specimens.

### 38.3.B. Inter- and Intra-Band Transitions

An electron in the beam may transfer sufficient energy to a core electron to cause it to change its orbital state, for example, to a Bohr orbit of higher quantum number. We call these events "single electron interactions" and they result in energy losses of up to ~25 eV. Interactions with molecular orbitals such as the  $\pi$  orbitals produce characteristic peaks in this low-energy region of the spectrum, and it is possible sometimes to use the intensity variation in this part of the spectrum to identify a particular specimen. However, the details of the spectrum intensity variations due to single electron interactions are not well understood and cannot yet be predicted *a priori*.

Use of the low-loss spectrum for phase identification is only possible through a "fingerprinting" process by which the low-loss spectra of known specimens are stored in a library in the computer.

Spectra from unknown specimens may then be compared with the stored library standards. Figure 38.3 shows the low-loss spectra of Al and Al-containing compounds exhibiting differences in the detailed intensity variation. A collection of low-loss spectra from all the elements has been compiled in the EELS Atlas (Ahn and Krivanek 1983) and this can help with "fingerprinting" unknown specimens.

If the beam electron gives a weakly bound valence-band electron sufficient energy to escape the attractive field of the nucleus, then we've created a secondary electron (SE), of the sort used to give topographic images in the SEM and STEM. Typically, we give <20 eV to a SE and therefore the electrons causing SE emission appear in the same low-energy region of the spectrum as the inter- and intra-band transitions.

The weakly bound outer-shell electrons control the reaction of an atom to an external field and thus control the dielectric response of the material. We'll see in Chapter 40 that it is possible to get a measure of the dielectric constant by careful processing of the very low loss portion (<~10 eV) of the spectrum.

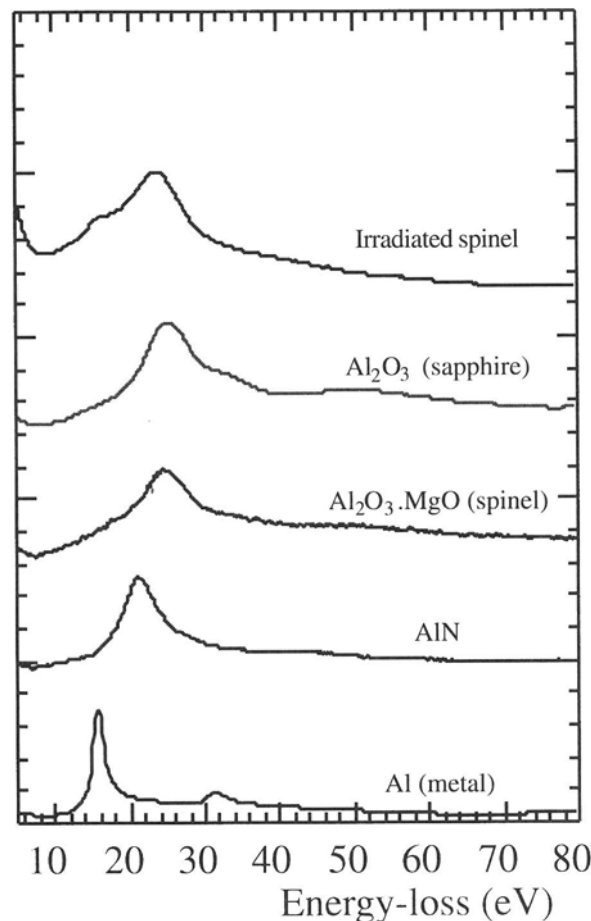


**Figure 38.3.** The low-loss spectrum from specimens of Al and Al-containing compounds, showing differences in intensity that arise from differences between the bonding in the different materials. The spectra are displaced vertically for ease of comparison.

## 38.4. THE HIGH-LOSS SPECTRUM

The high-loss portion of the spectrum above about 50 eV contains information from inelastic interactions with the inner or core shells.

### 38.4.A. Inner-Shell Ionization

When a beam electron transfers sufficient energy to a K, L, M, N, or O shell electron to move it outside the attractive field of the nucleus, as shown back in Figure 4.2, the atom is said to be ionized. As you know from the earlier chapters on X-ray analysis, the decay of the ionized atom back to its ground state may produce a characteristic X-ray, or an Auger electron. So the processes of inner-shell ionization-

loss EELS and XEDS are different aspects of the same phenomenon. We are interested in ionization losses precisely because the process is characteristic of the atom involved and so the signal is a direct source of elemental information, just like the characteristic X-ray. We call the ionization-loss signal an “edge” for reasons we’ll describe shortly.

You should appreciate that detection of the beam electron that ionized the atom is independent of whether the atom emits an X-ray or an Auger electron. EELS is not affected by the fluorescence-yield limitation that restricts light-element X-ray analysis. This difference explains, in part, the complementary nature of XEDS and EELS.

Inner-shell ionization is generally a high-energy process. For example, the lightest solid element, Li, requires an input of  $\geq 55$  eV to eject a K-shell electron, and so the loss electrons are usually found in the “high-loss” region of the spectrum, above  $\sim 50$  eV. K-shell electrons require much more energy for ejection as  $Z$  increases, because they are more strongly bound to the nucleus. The binding energy for electrons in the Uranium K shell is about 99 keV. So, as in XEDS, we tend to look for other lower-energy ionizations, such as the L and M edges, when dealing with high- $Z$  atoms. Typically, we start to use the L edges when the K-shell energy exceeds  $\sim 1$  keV (Na) and M edges when the L shell exceeds  $\sim 1$  keV (Zn).

It’s worth a short mention here about the nomenclature used for EELS edges. Just like in X-rays, where we have K, L, M, etc. peaks in the spectrum, we get ionization edges from K, L, M, etc. shell electrons. However, the greater energy resolution of the EELS spectrometer means that it is much easier to detect differences in spectra that arise from the presence of different energy states in the shell. For example:

- The K-shell electron is in the 1s state and gives rise to a single K edge.
- In the L shell, the electrons are in either 2s or 2p orbitals, and if a 2s electron is ejected, then we get an  $L_1$  edge, and a 2p electron causes either an  $L_2$  or  $L_3$  edge.

The  $L_2$  and  $L_3$  edges may not be resolvable at lower ionization energies (e.g., they aren’t in Al but they are in Ti), and sometimes we call this edge the  $L_{2,3}$ . The full range of possible edges is shown schematically in Figure 38.4, and you can see that other “dual” edges exist, such as the  $M_{4,5}$ . There will be more about this in Chapter 40.

Compared with plasmon excitation, which requires much less energy, the ionization cross sections are relatively small and the mean-free paths relatively large. As a result the ionization edge intensity in the spectrum is very much smaller than the plasmon peak, and becomes even smaller as the energy loss increases (look back to Figure 37.4A). This is another reason for staying with the lower-energy-loss (L and M) core edges. While the possibility of plural ionization events being triggered by the same electron is small in a typical thin foil, we’ll see that the combination of an ionization loss with a plasmon loss is by no means uncommon, and this phenomenon distorts the resultant spectrum.

If you go back and look at Figure 4.2, you can see that a specific minimum-energy transfer from the beam electron to the inner-shell electron is required to overcome the binding energy of the electron to the nucleus and ionize the atom.

This minimum energy constitutes the ionization threshold, or the critical ionization energy,  $E_C$ .

We define  $E_C$  as  $E_K$  for a particular K-shell electron,  $E_L$  for an L shell, etc. Of course, it is also possible to ionize an atom by the transfer of  $\mathcal{E} > E_C$ . However, the chances of ionization occurring become less with increasing energy above  $E_C$ , because the value of the cross section decreases with increasing energy. As a result, the ionization-loss electrons have an energy distribution that ideally shows a sharp rise to a maximum at  $E_C$ , followed by a slowly decreasing intensity above  $E_C$  back toward the background. This triangular shape is called an “edge.”

This idealized triangular or saw-tooth shape is only found in spectra from isolated hydrogen atoms, and is therefore called a hydrogenic ionization edge. Real ionization edges have shapes that approximate, more or less, to the hydrogenic edge.

You’ll notice that this edge, shown in Figure 38.5A, has almost the same intensity profile as the “absorption edges” in X-ray spectroscopy. In reality, because we aren’t dealing with isolated atoms but atoms integrated into a crystal lattice or amorphous structure, the spectra become more complex. The ionization edges are superimposed on a rapidly decreasing background intensity from electrons that have undergone random, plural inelastic scattering events (Figure 38.5B). The edge shape may also contain fine structure around  $E_C$  (Figure 38.5C) which is due to bonding effects, and is termed energy-loss near-edge structure (ELNES). More than  $\sim 50$  eV after the edge, small intensity oscillations may be detectable (Figure 38.5D) due to diffraction effects from the atoms surrounding the ion-

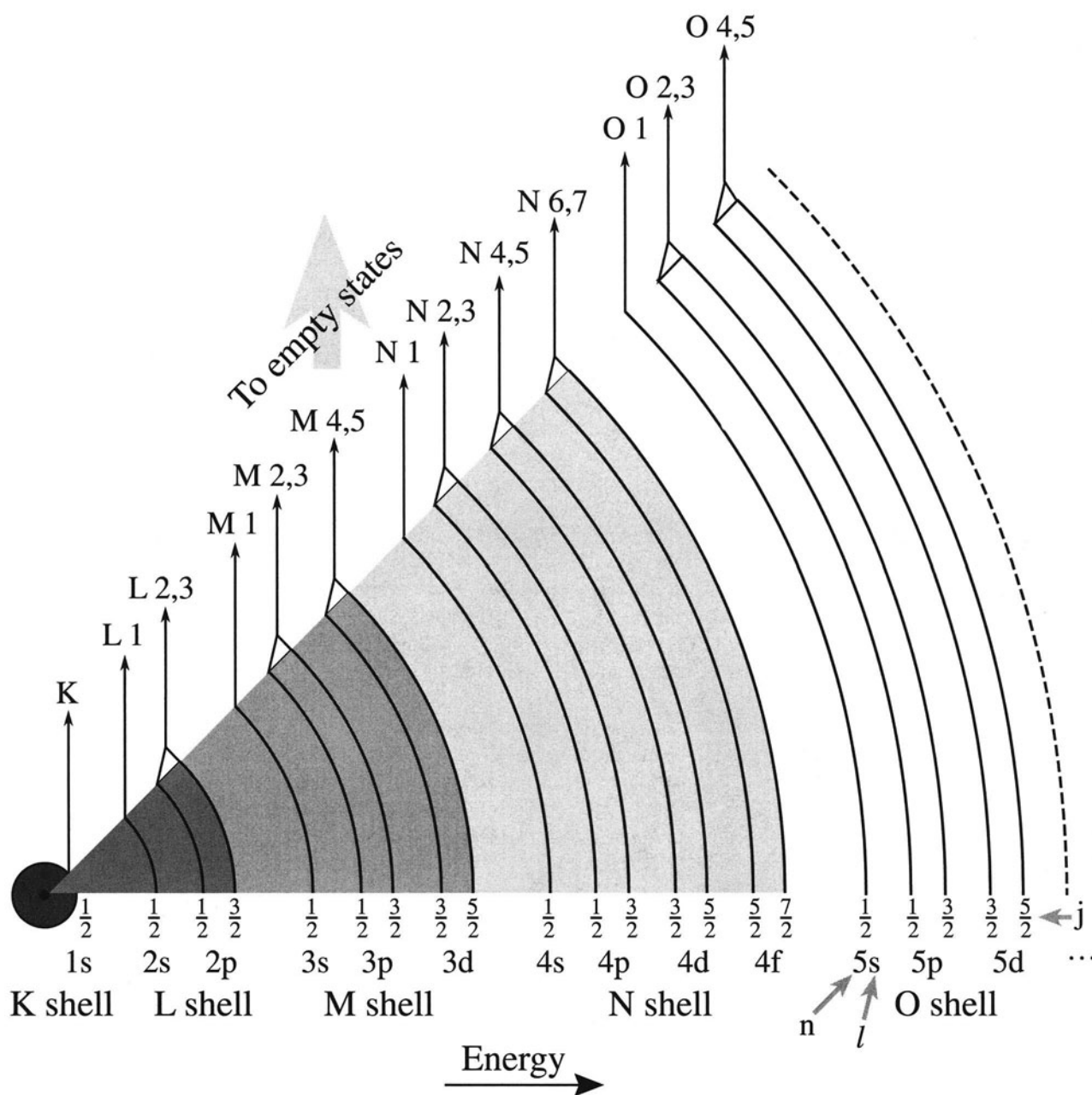


**Figure 38.4.** The full range of possible edges due to inner-shell ionization, and their associated nomenclature.

ized atom, and these oscillations are called extended energy-loss fine structure (EXELFS), which is analogous to extended X-ray absorption fine structure (EXAFS) in X-ray spectra, particularly those generated from intense synchrotron sources.

- Fine structure before or around the peak is known as ELNES.
- Small intensity oscillations  $> \sim 50$  eV after the edge due to diffraction effects are called EXELFS.

Finally, as we noted earlier, the ionization-loss electrons may also undergo further low-loss interactions. They may create plasmons, in which case the ionization edge contains plural scattering intensity  $\sim 15\text{--}25$  eV above  $E_C$ , as shown in Figure 38.5E. So the resultant ionization edge is far more complicated than the simple Gaussian peak seen in an XEDS spectrum. Clearly, the edge details contain far more information about the specimen than a characteristic X-ray peak. From an X-ray spectrum you only get *elemental* identification rather than *chemical* in-

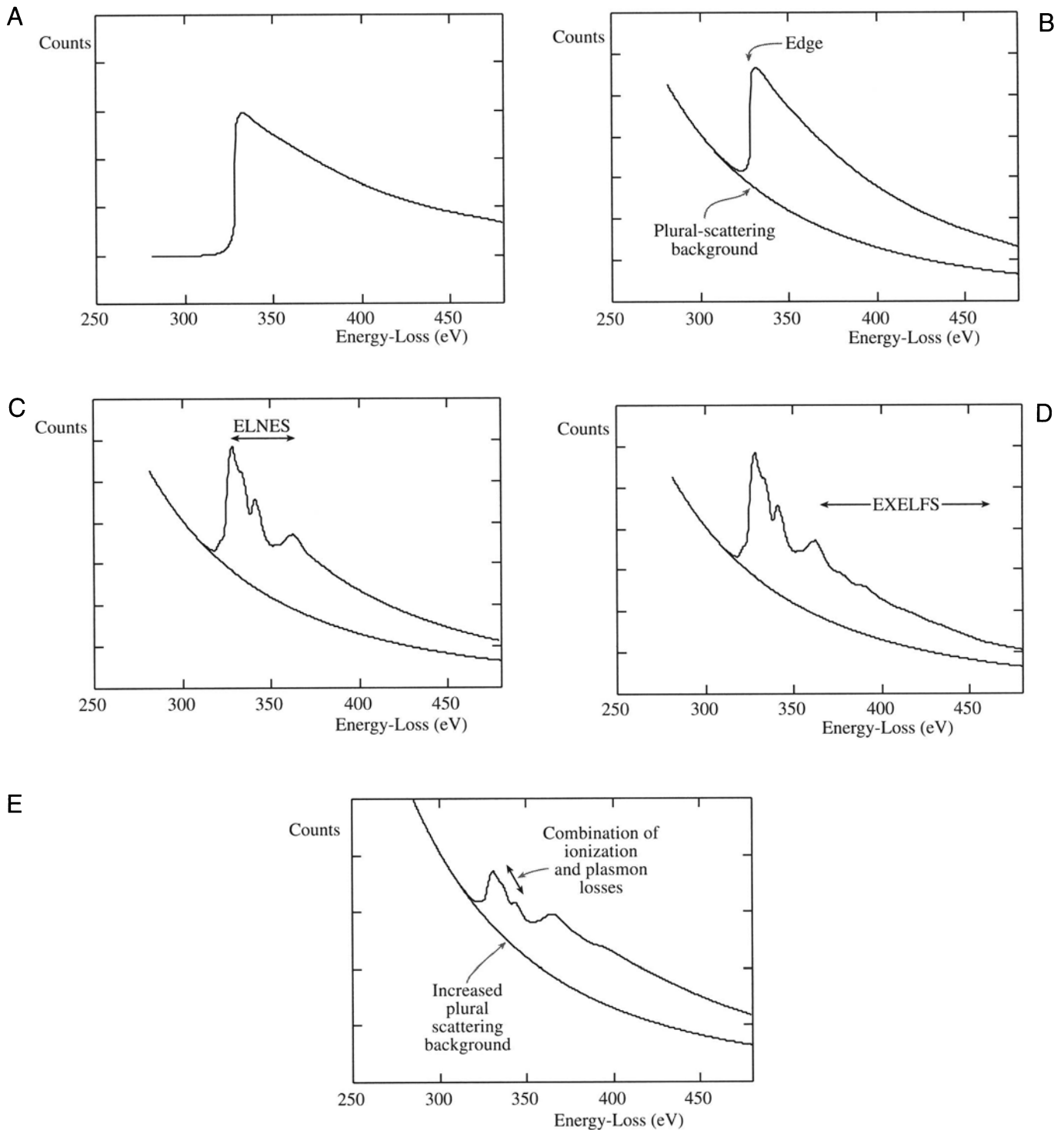


**Figure 38.5.** The characteristic features of an inner-shell ionization edge: (A) the idealized saw-tooth (hydrogenic) edge, (B) the edge superimposed on the background arising from plural inelastic scattering, (C) the presence of ELNES, (D) the EXELFS. (E) Plural scattering in a thick specimen, such as the combination of ionization and plasmon losses, distorts the post-edge structure and give an increase in the background level.

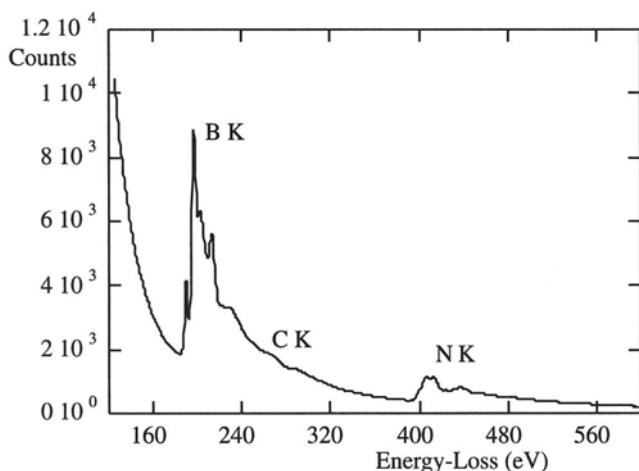


**Figure 38.6.** High-energy-loss spectrum from a particle of BN over a hole in a C film showing the B and N K-shell ionization edges superimposed on a rapidly decreasing background. A faint C K edge is also visible at  $\sim 280$  eV.

formation, such as bonding, which is contained in the ELNES. Figure 38.6 shows a spectrum from BN on a C film. The various ionization edges show some of the features drawn schematically in Figure 38.5; we'll discuss these "fine structure" effects more in Section 40.1.

### 38.4.B. Ionization-Edge Characteristics

The angular distribution of ionization-loss electrons varies as  $(\theta^2 + \theta_E^2)^{-1}$  and will be a maximum when  $\theta = 0^\circ$ , in the forward-scattered direction. The distribution decreases to a half width at the characteristic scattering angle  $\theta_E$  given by equation 38.1. This behavior is essentially the same as for plasmon scattering, but we have relatively large values of  $E_C$  compared to  $\mathcal{E}_p$ :

- $\theta_E \sim 5$  mrad for ionization-loss electrons at  $E_C = 1000$  eV, for a beam energy of 100 keV.
- The average plasmon-loss scattering was broadened to  $\sim 10$ –15 mrad.

The characteristic scattering angles for both plasmon and inner-shell ionization are still much lower than the characteristic scattering angles for phonon and elastic scattering. The angular distribution varies depending on the energy loss, and because of the extended energy range of ionization-loss electrons above  $E_C$ , this can be quite complicated. For  $\mathcal{E} \sim E_C$  the intensity drops rapidly to zero over about 10 mrad at  $\theta_C$ , but as  $\mathcal{E}$  increases above  $E_C$  the angular intensity distribution drops around  $\theta = 0^\circ$ , but increases at larger scattering angles, giving rise to the so-called Bethe Ridge. Since this effect is irrelevant for EELS studies, we'll ig-

nore it, but you can find more information in Egerton (1996).

So, in the region immediately following the ionization edge the angular distribution of the electrons is generally confined to a semiangle of  $<10$ –15 mrad and drops to zero beyond this. In other words, like the plasmon-loss electrons, the ionization-loss electrons are very strongly forward-scattered. Consequently, efficient collection of the major inelastically scattered electrons is a straightforward matter, since a spectrometer entrance aperture semiangle ( $\beta$ ) of  $<20$  mrad will collect the great majority of these electrons. As a result, collection efficiencies in the range 50–100% are not unreasonable, which contrasts with the situation in XEDS, where the isotropic generation of characteristic X-rays results in very inefficient collection. Figure 38.7 compares the collection of X-rays and energy-loss electrons in the AEM. Figure 38.8 shows the variation in collection efficiency for ionization-loss electrons as a function of both  $\beta$  and energy.

While the K edges in Figure 38.6 show reasonably sharp onsets, like an ideal hydrogenic edge, not all edges are similar in shape. Some edges have much broader onsets, spread over several eV or even tens of eV. The edge shape in general depends on the electronic structure of the atom but, unfortunately, we can't give a simple relationship between specific edge types and specific shapes. The situation is further complicated by the fact that the edge shapes change significantly depending on whether or not

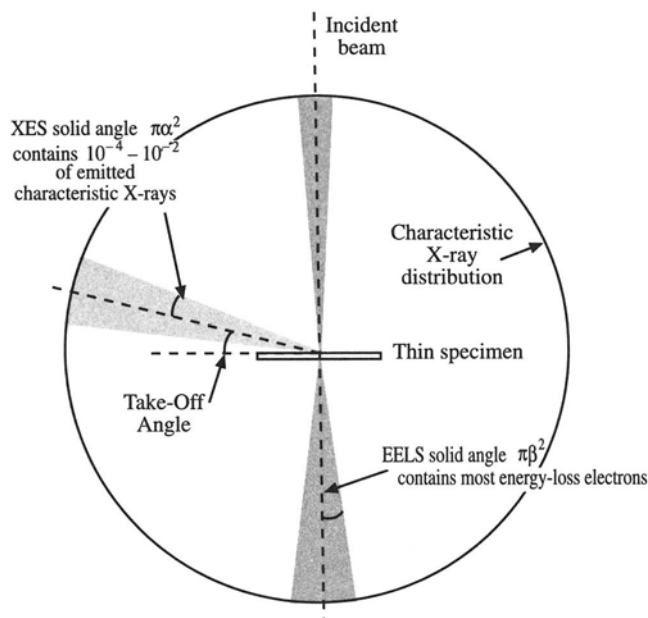


**Figure 38.7.** Comparison of the relative efficiencies of collection of EELS and XEDS. The forward-scattered energy-loss electrons are more efficiently collected than the uniformly emitted characteristic X-rays.

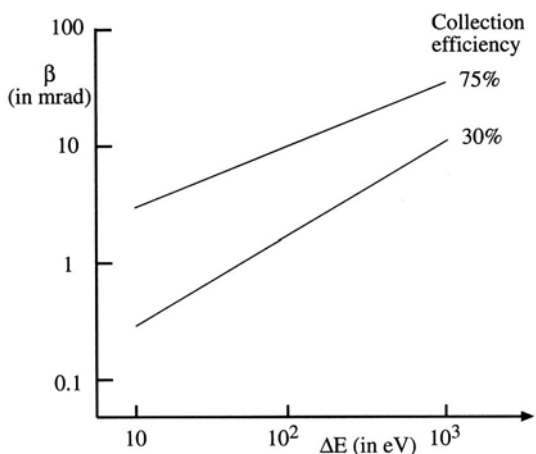


**Figure 38.8.** Variation in the collection efficiency of ionization-loss electrons as a function of their energy and the spectrometer collection semiangle,  $\beta$ .

certain energy states are filled or unfilled. For example, if you look below at Figure 38.9, the Ni L edge shows two sharp peaks, which are the  $L_3$  and  $L_2$  edges. (We'll discuss these details much more in Section 40.1.) These sharp lines arise because the ejected L shell electrons don't entirely escape from the atom and have a very high probability of ending up in unfilled d band states, which are present in Ni. In contrast, in Cu, in which the d band is full, the  $L_{2,3}$  edge does not show these intense lines. Similar sharp lines appear in the  $M_{4,5}$  edges in the rare earths. As if this were not enough, the details of the fine structure and edge shapes are also affected by bonding. For example, the Ni edge in NiO in Figure 38.9 is different from the Ni edge in pure Ni. To sort all this out it's best if you consult the EELS Atlas (Ahn and Krivanek 1983), which contains representative edges from all the elements and many oxides.

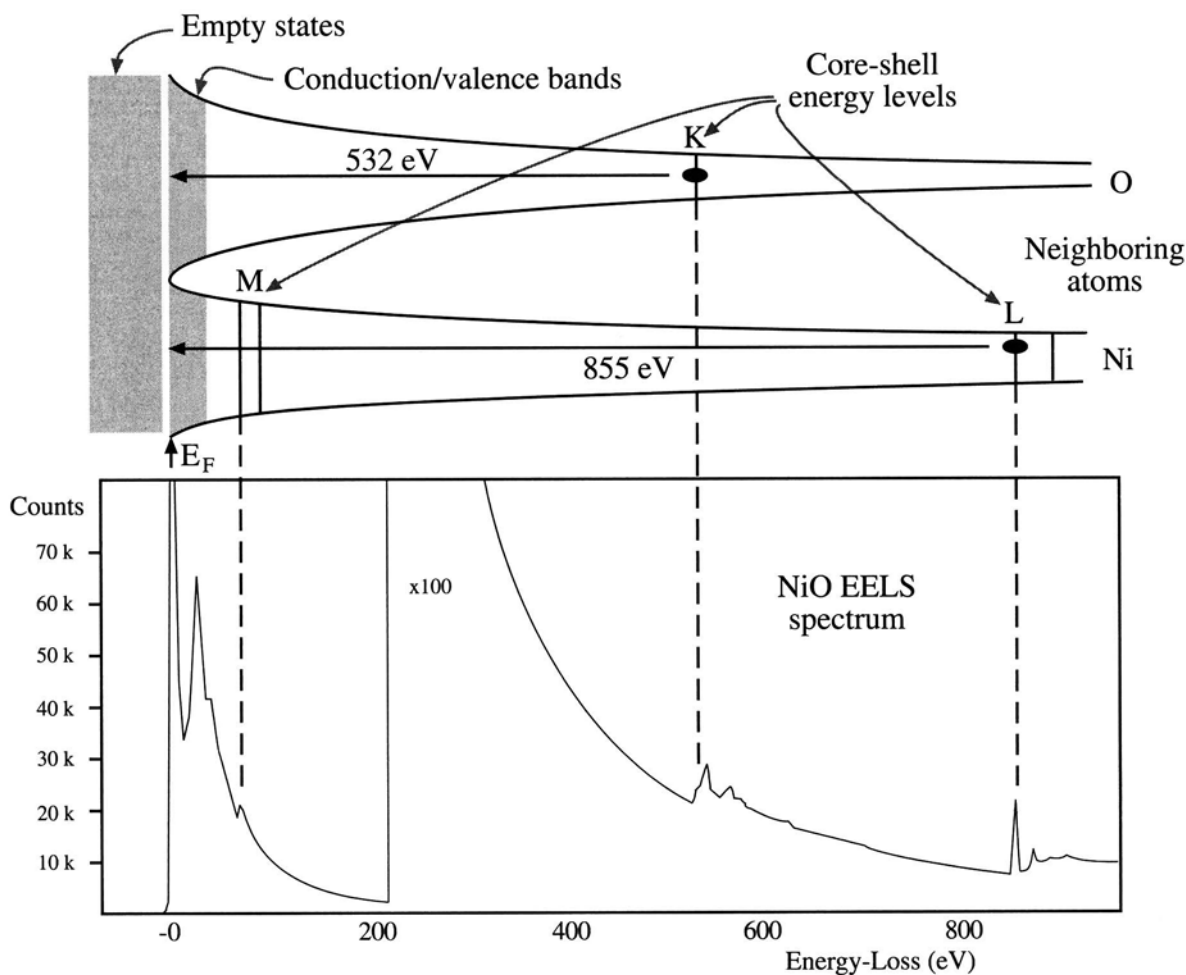


**Figure 38.9.** The correspondence between the energy levels of electrons surrounding adjacent Ni and O atoms and the energy-loss spectrum: the zero-loss peak is above the Fermi energy  $E_F$ , the plasmon peak is at the energy level of the conduction/valence bands, and the critical ionization energy required to eject specific K-, L-, and M-shell electrons is shown.

We can summarize the characteristics of the energy-loss spectrum by showing a complete spectrum from NiO containing both low- and high-loss electrons, as shown in Figure 38.9. In this figure we also compare the spectrum to the energy-level diagram for NiO. You can see that:

- The plasmon peak corresponds to the energy of the valence electron band just below the Fermi level ( $E_F$ ).
- The relative energy levels of the ionized atom (K, L, or M) control the position of the ionization edge in the spectrum.
- The different density of states in the valence (3d) band of the Ni atom is indicated by shading at the top of the potential wells and is reflected in the characteristic, intense, near-edge, fine structure at the Ni L edge.

The electrons could also be given sufficient energy to travel into the conduction band well above  $E_F$ ; as we just mentioned, in this case we see extended fine structure after the ionization edge. We'll discuss more details of such fine structure in the spectrum in Chapter 40.

Despite the very high collection efficiency of the spectrometer, the ionization edges, which are the major signal for elemental analysis, show relatively low intensity, have an extended energy range above the ionization energy, and ride on a rapidly varying, relatively high background. All these factors, as we shall see, combine to make quantitative microanalysis using EELS a difficult and less accurate technique when compared with XEDS. However, for the light elements the X-ray fluorescence yield drops to such low values, and absorption becomes so strong, even in thin specimens, that EELS is the preferred technique. Experimentally, the choice between the two is not simple, but below oxygen in the periodic table, EELS has shown better performance than XEDS and, for elements below boron, there is no sensible alternative to EELS for microanalysis at high spatial resolution.

### 38.5. ARTIFACTS IN THE SPECTRUM

The SEELS spectrum contains no artifacts of any consequence, unless it is grossly misaligned, in which case the beam may scatter through the slits or off the drift tube, giving distorted background intensities. These effects are easy to spot and correct.

Unfortunately, the highly efficient PEELS system generates more artifacts which you have to recognize and remove before analyzing the spectrum. Details are available in the Gatan manual, but here we'll summarize

the major problems (which are in addition to the point-spread function that we talked about in the previous chapter).

All the individual diodes will differ slightly in their response to the incident electron beam, and therefore there will be a channel-to-channel gain variation in intensity. This will be characteristic of each individual diode array.

One way to determine the gain variation is to spread the beam uniformly over the array using at least the 3-mm entrance aperture and looking at the diode readouts, as shown in Figure 38.10. This is difficult with an FEG system because the probe is too small, and then it is necessary to scan the beam across the array, although this is not very satisfactory. Then you have to divide your experimental spectrum by this response spectrum to remove the gain variation. Alternatively, and this is recommended, you can gather two or more spectra with slight energy shifts ( $\sim 1$ – $2$  eV) or spatial shifts between them and superimpose them electronically. The gain variation then disappears, as you can see if you look at Figure 38.12. Using a two-dimensional array, as in the GIF, removes this problem also.

Gathering many spectra and superimposing them can bring another problem, namely, that of readout noise. There are two kinds of readout noise, random and fixed. The random readout noise, or shot noise, arises from the electronics chain from the diode to the display, and is minimized by taking as few readouts as possible, and also by

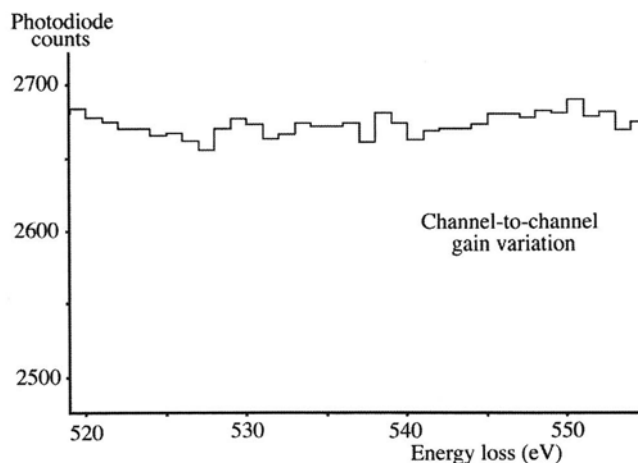


**Figure 38.10.** The variation in the response of individual diodes in the PEELS detection system to a constant incident electron intensity. A channel-to-channel gain variation is clear and each detector array has its own characteristic response function.

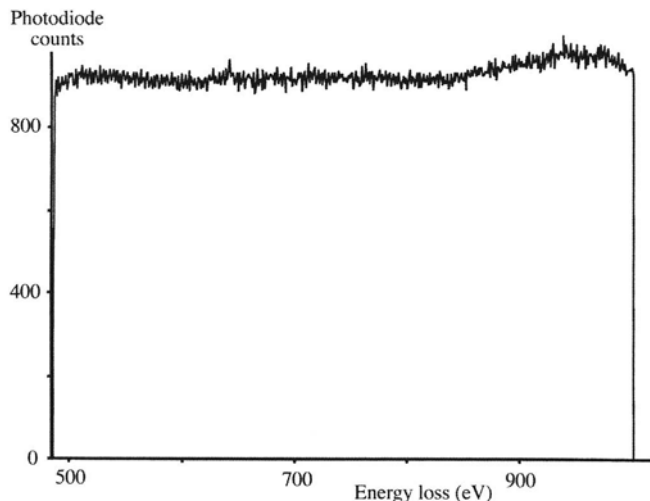


**Figure 38.11.** The intensity of the dark current which flows from the diode array when no electron beam is present.

cooling the diode array. Individual diodes may have high leakage currents which give a spike on the display. The fixed pattern readout noise is a function of the three-phase readout circuitry. All these effects will appear when there is no current falling on the diodes and together they constitute the dark current (see Figure 38.11). The dark current is small unless you have a bad diode array, and it is only a problem when there are very few counts in your spectrum or you have added together 10 or more spectra. Figure 38.12 shows some of these effects and how to remove them.

Finally, there is the problem of incomplete readout of the display. When the diodes are cooled, only ~95% of the signal is read out in the first integration, ~4.5% in the second, ~0.25% in the third, and so on. This is only a problem if you have saturated the diodes with an intense signal like the zero-loss peak. This peak then shows up as a ghost peak in the next readout and decays slowly over several readouts. So if a ghost peak appears, just run several readouts and it will disappear; this way you should never confuse a ghost peak with a genuine edge.

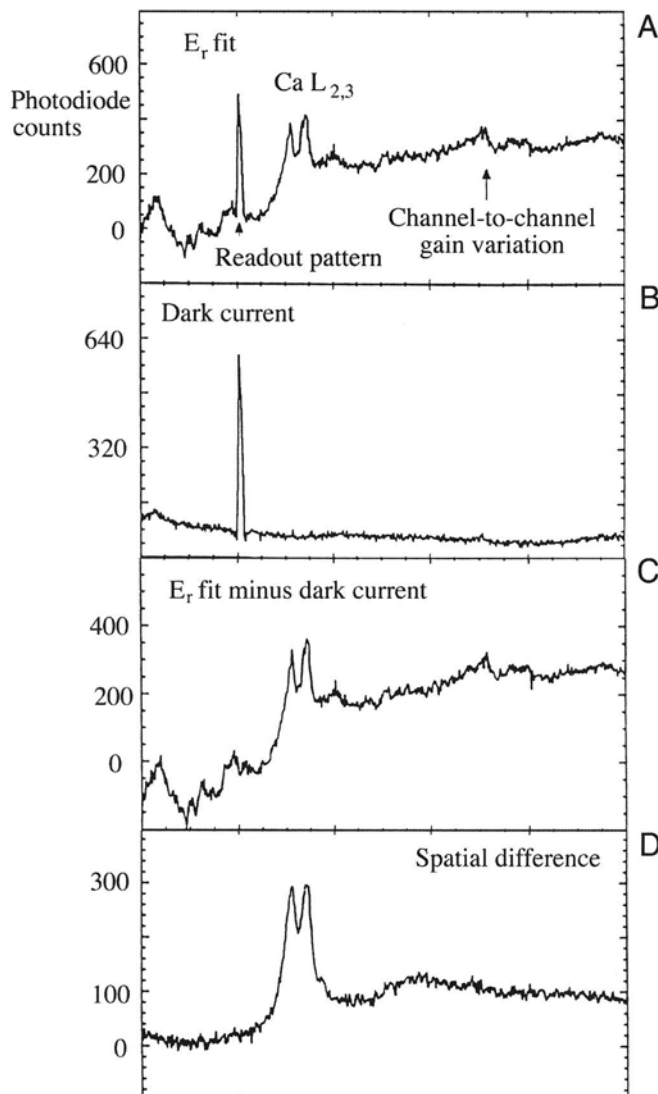


**Figure 38.12.** How to remove artifacts from a specimen: (A) A  $\text{Ca L}_{2,3}$  edge spectrum showing both channel-to-channel gain variation and a faulty diode with a high leakage current which appears as a spike in the spectrum. The spike is referred to as the readout pattern and is present in every recorded spectrum. Subtracting the dark current (B) removes the spike (C) and a difference spectrum (D) removes the gain variation, leaving the desired edge spectrum.

## CHAPTER SUMMARY

The EELS spectrum varies in intensity over several orders of magnitude.

- The least useful signal (the zero-loss peak) is the most intense, and the most useful signals (the ionization edges) are among the least intense signals.
- The low-loss spectrum reflects beam interactions with loosely bound conduction and valence-band electrons.

**Table 38.3. PEELS Artifacts and How to Eliminate Them**

Noise name	Source	Elimination
Leakage current	Different diodes	Subtract dark current
Internal scanning noise	Electronics readout	Adjust the electronics and subtract the dark count
Nonuniform sensitivity	Diode sensitivities differ	Determine the response characteristic by sweeping the beam along the array and divide the real spectrum by this result, i.e., normalize the diodes

- The high-loss spectrum contains small ionization edges riding on a strong plural-scattered background.
- Differences in the energy onset of the ionization edges distinguish different elements in the specimen.
- Differences in the fine structure of the edges reflect chemical (bonding) effects and structural (atomic arrangement) effects.
- Artifacts can complicate spectrum interpretation, but they are well understood and easily removed.

We summarize the different sources of noise and how we eliminate this noise in Table 38.3.

## REFERENCES

### Specific References

- Egerton, R.F. (1996) *Electron Energy Loss Spectroscopy in the Electron Microscope*, 2nd edition, Plenum Press, New York.
- Ahn, C.C. and Krivanek, O.L. (1983) *EELS Atlas*, Gatan Inc., 780 Commonwealth Drive, Warrendale, Pennsylvania.